# Application of cooled spatial light modulator for high power nanosecond laser micromachining

# Application of cooled spatial light modulator for high power nanosecond laser micromachining

**Rainer J Beck,[1,*] Jonathan P Parry,[1] William N MacPherson,[1] Andrew Waddie,[1] Nick J Weston,[2] Jonathan D Shephard,[1] and Duncan P Hand[1]**

[1]*School of Engineering and Physical Sciences, Heriot-Watt University, Edinburgh, EH14 4AS, UK*
[2]*Renishaw plc, Heriot-Watt Research Park North, Riccarton, Edinburgh EH14 4AP, UK*
**rjb8@hw.ac.uk*

**Abstract:** The application of a commercially available spatial light modulator (SLM) to control the spatial intensity distribution of a nanosecond pulsed laser for micromachining is described for the first time. Heat sinking is introduced to increase the average power handling capabilities of the SLM beyond recommended limits by the manufacturer. Complex intensity patterns are generated, using the Inverse Fourier Transform Algorithm, and example laser machining is demonstrated. The SLM enables both complex beam shaping and also beam steering.



**OCIS codes:** (230.6120) Spatial light modulators; (140.3390) Laser materials processing; (050.1970) Diffractive optics.

## References and links

1. S. Campbell, S. M. F. Triphan, R. El-Agmy, A. H. Greenaway, and D. T. Reid, "Direct optimization of femtosecond laser ablation using adaptive wavefront shaping," J. Opt. A, Pure Appl. Opt. **9**(11), 1100–1104 (2007).
2. R. Beck, R. Carrington, J. Parry, W. MacPherson, A. Waddie, D. T. Reid, N. Weston, J. Shephard, and D. P. Hand, "Adaptive optics for optimization of laser processing," in Proc. of LAMP2009 (Japan, 2009).
3. V. Laude, "Twisted-nematic liquid-crystal pixelated active lens," Opt. Commun. **153**(1-3), 134–152 (1998).
4. E. Martín-Badosa, M. Montes-Usategui, A. Carnicer, J. Andilla, E. Pleguezuelos, and I. Juvells, "Design strategies for optimizing holographic optical tweezers set-ups," J. Opt. A, Pure Appl. Opt. **9**(8), S267–S277 (2007).
5. K. D. Wulff, D. G. Cole, R. L. Clark, R. Dileonardo, J. Leach, J. Cooper, G. Gibson, and M. J. Padgett, "Aberration correction in holographic optical tweezers," Opt. Express **14**(9), 4169–4174 (2006).
6. P. M. Prieto, E. J. Fernández, S. Manzanera, and P. Artal, "Adaptive optics with a programmable phase modulator: applications in the human eye," Opt. Express **12**(17), 4059–4071 (2004).
7. L. Kelemen, S. Valkai, and P. Ormos, "Parallel photopolymerisation with complex light patterns generated by diffractive optical elements," Opt. Express **15**(22), 14488–14497 (2007).
8. Z. Kuang, W. Perrie, J. Leach, M. Sharp, S. P. Edwardson, M. Padgett, G. Dearden, and K. G. Watkins, "High throughput diffractive multi-beam femtosecond laser processing using a spatial light modulator," Appl. Surf. Sci. **255**(5), 2284–2289 (2008).
9. D. Liu, Z. Kuang, S. Shang, W. Perrie, D. Karnakis, A. Kearsley, M. Knowles, S. Edwardson, G. Dearden, and K. Watkins, "Ultrafast parallel laser processing of materials for high throughput manufacturing," in Proc. of LAMP2009 (Japan, 2009).
10. S.-W. Bahk, E. Fess, B. E. Kruschwitz, and J. D. Zuegel, "A high-resolution, adaptive beam-shaping system for high-power lasers," Opt. Express **18**(9), 9151–9163 (2010).
11. P. Gerets, K. Vandorpe, and W. Van Rafelgem, "Cooling of reflective spatial light modulating devices," US Pat. 2008/0024733 A1 (Jan. 31. 2008).
12. G. Stoilov, and T. Dragostinov, "Phase-stepping interferometry: Five-frame algorithm with an arbitrary step," Opt. Lasers Eng. **28**(1), 61–69 (1997).
13. J. Otón, P. Ambs, M. S. Millán, and E. Pérez-Cabré, "Multipoint phase calibration for improved compensation of inherent wavefront distortion in parallel aligned liquid crystal on silicon displays," Appl. Opt. **46**(23), 5667–5679 (2007).
14. I. Moreno, A. Lizana, A. Márquez, C. Iemmi, E. Fernández, J. Campos, and M. J. Yzuel, "Time fluctuations of the phase modulation in a liquid crystal on silicon display: characterization and effects in diffractive optics," Opt. Express **16**(21), 16711–16722 (2008).
15. A. Hermerschmidt, S. Osten, S. Krüger, and T. Blümel, "Wave front generation using a phase-only modulating liquid-crystalbased micro-display with HDTV resolution," in Proc. SPIE (2007).
16. F. Wyrowski, and O. Bryngdahl, "Iterative Fourier-Transform Algorithm Applied to Computer Holography," J. Opt. Soc. Am. A **5**(7), 1058–1065 (1988).

#130546 - $15.00 USD Received 22 Jun 2010; revised 16 Jul 2010; accepted 19 Jul 2010; published 27 Jul 2010

## 1. Introduction

Nanosecond lasers enable high-precision machining of a wide range of materials with a comparatively high throughput. It is well known that the typical Gaussian intensity distribution generated at focus is not always ideal for the application. Deformable mirrors are a robust and fast (typical response time of ≥ 1 ms) approach to modify the beam shape for laser machining applications [1,2]; however common commercially available devices have a comparatively small number of active elements, typically only 37 elements although devices with more actuators are available, e.g. by ALPAO; as a result the degree of control of beam shape that can be achieved is rather limited. Devices with higher numbers of actuators are fairly expensive therefore limiting their potential application for laser micromachining in industrial processes. Spatial light modulators (SLM) based on liquid crystal displays are a highly competitive alternative. They provide increased flexibility due to their large number of small pixels (typically > 250,000) and are easily programmable. Consequently, they have been applied to a variety of beam shaping applications such as programmable lenses [3], optical tweezers [4,5] or adaptive optics [6]. They do have disadvantages in comparison with deformable mirrors as they are slower, and have a lower average power optical damage threshold (although they can cope with high peak powers [7,8]). As a result, research into SLMs for micromachining of metals, polymers and silicon has been limited to femtosecond [7,8] and picosecond [9] laser pulses where the average powers required are relatively low. However, in industry nanosecond pulsed laser machining is more common. Hence there is a significant driver for the work presented in this paper particularly if SLMs are to be considered for development of practical laser machining applications. An SLM has been applied recently for high peak power nanosecond beam shaping but using a nanosecond laser source with a much shorter pulse length and much lower average power [10]. A cooling comprising housing of a reflective SLM has been patented for application in projectors [11].

We present in this paper the application of the spatial light modulator LC-R 2500 manufactured by Holoeye in nanosecond laser machining of a polyimide and a metal film, to our knowledge the first report of an SLM operating in this regime with high average power. The SLM works in reflection and has a resolution of 1024 x 768 pixels in a dimension of 19.5 x 14.6 mm. The power handling capabilities of the SLM display are stated by the manufacturer to be 1-2W/cm$^2$, limiting the total average power to about 3W assuming a circular laser beam with a diameter of 14mm at normal incidence on the display. However, for the majority of standard nanosecond laser machining processes somewhat higher laser powers are required.

A heat sinking method is applied to the SLM which enables the display to cope with higher average laser powers and results of experiments to determine the damage threshold are presented. Finally, laser machining with a complex beam shape is demonstrated.

## 2. Experimental configuration

### *2.1 Phase-stepping interferometer*

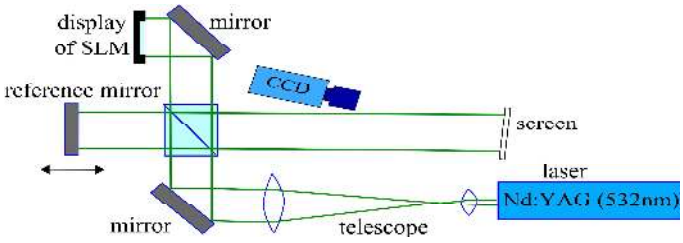


Fig. 1. Setup of phase-stepping interferometer.

A phase-stepping interferometer (Fig. 1) was constructed to measure the surface shape of the SLM display. The interferometer is a Michelson arrangement and uses a frequency doubled

#130546 - $15.00 USD Received 22 Jun 2010; revised 16 Jul 2010; accepted 19 Jul 2010; published 27 Jul 2010

Nd:YAG laser source with a wavelength of 532nm, the same wavelength used for the laser machining experiments. The flat reference mirror in one arm of the Michelson interferometer is mounted on a computer-controlled piezoelectric translation stage to enable phase-stepping. This mirror is moved to five equidistant positions for the measurement and an intensity image is captured of each resulting fringe pattern using a monochrome CCD camera. Using the corresponding algorithm [12] and a standard phase unwrapping technique, the height profile of the reflective object, in this case the display of the SLM, located at the second interferometer arm can be determined.

*2.2. Laser machining setup*

The SLM was embedded into our nanosecond laser machining workstation. The laser is a pulsed Nd:$YVO_4$ system (Spectra-Physics Inazuma) at a wavelength of 532nm with a pulse length of 65ns and a repetition rate between 15 and 100 kHz. A telescope arrangement is used to increase the laser beam diameter to match the dimensions of the SLM display. The incoming laser beam is incident on the SLM at an angle of 10°. The orientation of the linear polarized light incident on the SLM is controlled by a half wave plate. After the SLM a second telescope and a flat field lens (f-theta lens) are used in a 6-f arrangement to reduce the beam diameter and to focus the laser beam onto the workpiece (see Fig. 2).

The display of the SLM is attached to a custom designed copper mount acting as a heat sink and enabling additional water cooling. Good thermal conductivity between the metal plate at the back of the SLM display and the copper mount was attained by grinding and polishing the copper surface close to optical flatness. The metal plate at the back of the SLM display is not polished. No further reduction of the surface roughness was possible due to the plastic housing covering the metal plate at the corners of the display. However, this was alleviated by applying a slide of Liquid Metal™ from Coollaboratory (often used in CPU cooling units) between the display and the copper block.

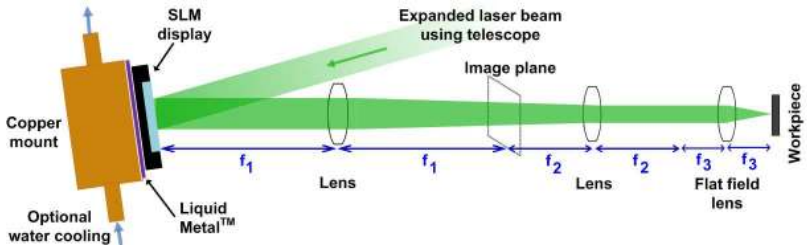


Fig. 2. Setup for laser machining experiments (SLM and copper mount shown enlarged).

## 3. Experimental results

*3.1 Curvature of display*

The display of the SLM exhibits an intrinsic curvature causing optical aberrations of the beam. The manufacturing process of the silicon backplane including the driving circuitry is based on standard CMOS processes [4] which are not optimised for high optical flatness. This is a well known problem for this type of device. In [4] a Fresnel lens phase map is successfully applied to the SLM in order to compensate for the curvature. A similar approach is essential here. The desired phase profile must be superimposed onto this compensational pattern with periodic boundary conditions between the gray values of the SLM corresponding to a phase change of $2\pi$. Figure 3a shows the initial surface height map of the SLM display obtained using phase-stepping interferometry as described in section 2.1. The display was attached to the mount supplied by the manufacturer and was switched off during the measurement. Since the display is relatively thin and quite flexible, the curvature varied significantly even for small changes in the way it is mounted. For our further experiments, the display was attached to a custom designed copper mount having a polished and flat surface

#130546 - $15.00 USD Received 22 Jun 2010; revised 16 Jul 2010; accepted 19 Jul 2010; published 27 Jul 2010

profile as described earlier. The display is mounted to the copper block using four screws located at the corners of the housing of the display. By adjusting these screws carefully and monitoring the shape of the display by means of the phase-stepping interferometer the device was flattened (see Fig. 3b). Based on the height data of the remaining surface deformation a wrapped phase map could be calculated and addressed to the SLM for compensation of the residual distortion. For our applications, as described below, a circular beam was incident to the central region of the "flattened" display fulfilling our criteria for the optical flatness (the root mean square deviation of this area was reduced by a factor of 3), therefore no additional compensational phase map is required in this case.

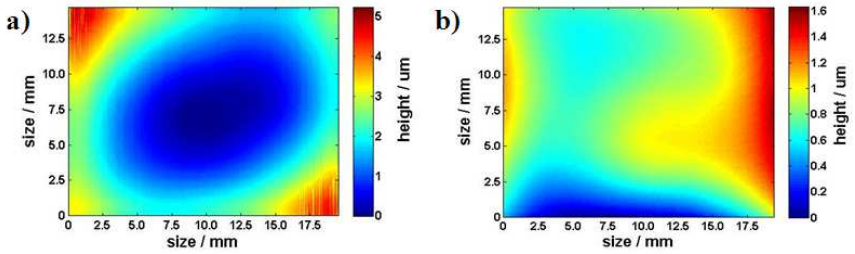


Fig. 3. Curvature of SLM display: a) initially; b) after mounting onto the copper mount; both height profiles determined experimentally using 5-step phase-stepping interferometry (small phase noise can result in vertical lines due to a spatial phase unwrapping technique).

### *3.2 Calibration of the phase response*

Due to the strain introduced by the four adjustment screws the relationship between the addressed pixel value and the resulting phase change needs to be recalibrated in order to ensure a linear response for the phase modulation between 0 and $2\pi$. In contrast to the phase-stepping technique, as described above and shown in Fig. 1, the flat reference mirror stays fixed for these measurements. Also, the display of the SLM is tilted resulting in a higher number of interference fringes. The calibration of the response of the SLM display is carried out based on phase shift interferometry as described in [13]. Initially, the look-up table (LUT) of the SLM, which determines the relationship between the addressed gray value and the resulting electric field across the liquid crystal, is set to a linear trend between the minimum and the maximum values for the available index values. Based on the measurement of the relative change of the fringe patterns (example fringe pattern shown in Fig. 4b) when altering half of the display between all available index values (Fig. 4a) a new look-up table can be calculated resulting in a near linear phase response (Fig. 4c). In [13], for a different kind of liquid crystal display, varying responses depending on the position on the display are reported and a local LUT in addition to the global LUT is suggested to overcome this issue. For the Holoeye LC-R 2500 no significant variations of the response for different positions were observed (see Fig. 4c).

#130546 - $15.00 USD Received 22 Jun 2010; revised 16 Jul 2010; accepted 19 Jul 2010; published 27 Jul 2010

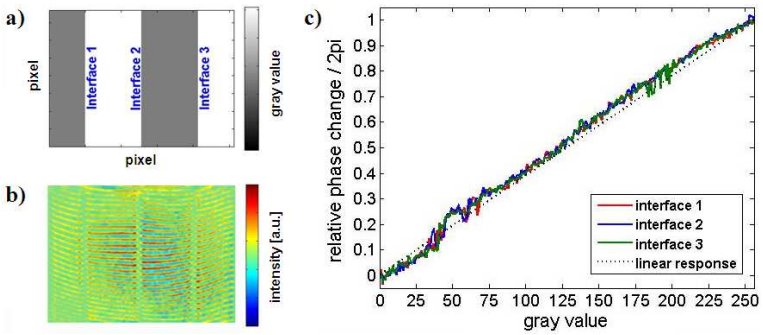


Fig. 4. a) Phase pattern addressed to the SLM; b) resulting interference pattern; c) phase responses for different areas on the SLM after calibration.

### *3.3 Power handling measurement*

The majority of nanosecond laser machining processes require a higher average power than the power handling capabilities stated by Holoeye for this device, i.e. 3W for a circular beam. Successful applications of this device for femtosecond processes as reported by [7,8] demonstrate that the high peak intensities in the ultrafast regime did not cause damage to the display. However, the absorbed heat over time can adversely affect the response of the display and potentially damage both the liquid crystal layer and the electronic driving circuitry on the silicon layer. The reflectivity of the display in this case is ~75% according to the display manufacturer Philips, therefore some incident light is absorbed by the device.

In order to examine the maximum power threshold of the device the SLM was incorporated into our nanosecond laser machining workstation as described in section 2.2. For this experiment, the laser beam is attenuated using a beam tap after the final focussing lens (see Fig. 2) and focussed onto a CCD camera. The intensity distribution in the zero order and in the first diffraction orders when addressing a simple binary grating onto the SLM was monitored over time for increasing laser powers. The phase difference of the binary grating was chosen to be less than $\pi$ resulting in the first diffraction orders and the zero order having similar intensities. According to the manufacturer small changes in this intensity distribution and thus the diffraction efficiency due to the absorbed heat in the display are reversible and do not cause permanent damage to the device. For the initial experiments the copper mount acted as a passive heat sink and no additional water cooling was used. We demonstrated that the SLM can withstand nanosecond laser pulses with 14.7W average power at a repetition rate of 30kHz over a timescale of 24 minutes without significant changes of the zero and first diffraction order intensities (Fig. 5a). The fluctuation of the diffraction efficiency, i.e. intensity ratio between the first diffraction orders and the zero order, over several minutes (as shown in Fig. 5b) is associated with variation in ambient air temperature in the lab. This is caused by the air conditioning system switching on and off. The temperature of the front surface of the display, measured using a pyrometer, increased to 48°C during the experiment. The drift of the diffraction efficiency as shown in Fig. 5b from ~1.25 to ~1.15 can be associated to this heating up of the device. The intensity values for the first diffraction orders are slightly different. This is caused by a consistent experimental error due to taking a point measurement within a finite size spot on the CCD camera. In a further experiment, the display of the SLM was exposed to the maximum average power of our laser, i.e. 14.7W, over a timescale of 60 minutes without damage to the device and without significant change in the diffraction efficiency.

The data shown in Fig. 5 captured with a standard CCD camera appear fairly noisy despite the binary grating being addressed continuously to the SLM. Indeed, it is the pulse width modulated signal from the control electronics to drive the pixels of the SLM display giving rise to these fluctuations as reported by [14] and [15].

#130546 - $15.00 USD Received 22 Jun 2010; revised 16 Jul 2010; accepted 19 Jul 2010; published 27 Jul 2010

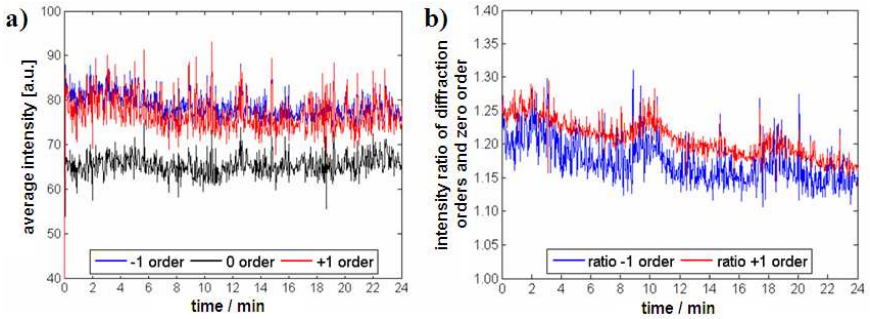


Fig. 5. a) temporal variation of intensity distribution in zero order (black line) and the first diffraction orders (blue and red line) with 14.7W average power being incident on the SLM display (~65ns pulse length; 30kHz repetition rate); b) intensity in the first diffraction orders divided by intensity of zero order.

### *3.4 Example laser machining*

The SLM in the optical arrangement described in this paper is working as a programmable diffractive optical element, and as such can generate a huge range of complex beam shapes. These beam shapes can then be used to directly machine complex patterns, without the need for beam scanning equipment. The increased power handling capabilities of this device when mounted onto the copper block enable nanosecond laser machining with complex intensity distributions. As an example a computer generated hologram (kinoform) of a "smiley face" was calculated using an Inverse Fourier Transform Algorithm (IFTA) [16] and addressed to the SLM. Figure 6a shows the laser machining result (repetition rate 30kHz, average power 14.7W, machining time 100ms) for a laser ablation process of a metal coated glass slide. The target for the IFTA was set off-axis in order to separate between the intended diffraction pattern and the zero order as seen in the bottom right corner of Fig. 6a. This approach enables both beam shaping and also beam steering as demonstrated in Fig. 6b: six individual kinoforms for a circular, a triangular, a doughnut and square target profiles at different locations were generated using the IFTA and laser machined sequentially (repetition rate 30kHz, average power 14.7W, machining time 3.2ms each) as an ablation process on polyimide coated metal. The different positions were achieved by means of the SLM rather than a mechanical beam scanning system. There is a strong mark at the centre of the top middle square of Fig. 6b caused by the zero order beam, which could be removed for instance by spatial filtering. Both laser machining results suffer from some speckle, e.g. a speckle may be around 1/6 of the size of a square, i.e. around 60µm, as shown in Fig. 6b. This is a known problem with the IFTA approach due to the discrete and finite pixel grid of the SLM display and hence limits the resolution on the features that can be produced.

#130546 - $15.00 USD Received 22 Jun 2010; revised 16 Jul 2010; accepted 19 Jul 2010; published 27 Jul 2010

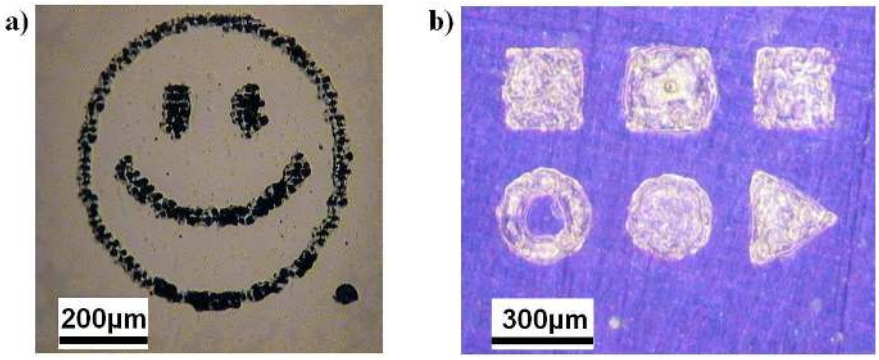


Fig. 6. Example laser machining: a) on metal coated glass slide using single diffraction pattern addressed to SLM based on Inverse Fourier Transform Algorithm (IFTA); b) on polyimide coated metal using a sequence of six individual IFTA generated kinoforms. Local positioning is achieved by the kinoform addressed to the SLM rather than a mechanical motion system.

## 4. Conclusion

We demonstrated that cooling of the display of the spatial light modulator LC-R 2500 enables the device to be applied for beam shaping for nanosecond laser machining with a much higher average power than recommended by the manufacturer. Utilizing the full resolution of the display, e.g. using an IFTA approach, complex intensity distributions can be generated having sufficient intensity for direct laser ablation. This adds an increased flexibility and process control to the nanosecond laser machining workstation.

**Acknowledgements**

This work was also funded by the UK Engineering and Physical Sciences Research Council, EPSRC. A special thanks to our industrial collaborator Renishaw plc for their funding, support and input. Many thanks also to Holoeye Photonics AG, via Stefan Osten, for their support.

#130546 - $15.00 USD Received 22 Jun 2010; revised 16 Jul 2010; accepted 19 Jul 2010; published 27 Jul 2010